Geomagnetic Diurnal Variation Modeling and Signal Extraction

Ningrui Li [#], Mingyu Wang [#], Yuanhang Bao [#, *]

Glasgow College Hainan, University of Electronic Science and Technology of China, Lingshui, China, 572400

* Corresponding Author Email: 2022360902038@uestc.edu.cn

[#]These authors contributed equally.

Abstract. This manuscript presents a comprehensive approach to geomagnetic field analysis, focusing on multi-sensor calibration, target signal isolation, and noise reduction. A diurnal geomagnetic variation model is introduced to calibrate multi-sensor data, addressing nonlinear trends and enhancing consistency across sensors. The model utilizes polynomial fitting and outlier removal to ensure accurate data. A novel technique for isolating the magnetic signal of a target object is developed by subtracting the reference signal and applying Savitzky-Golay filtering. Simulation results validate the effectiveness of the proposed methods, showing significant improvements in signal accuracy and robustness. This approach lays the groundwork for future research in geomagnetic data analysis, offering a reliable method for extracting target object signals in the presence of noise and sensor errors.

Keywords: Neural Geomagnetic Field Measurement, Multi-Sensor Calibration, Target Signal Separation, Filtering Processing, Savitzky-Golay.

1. Introduction

In recent years, due to various influencing factors, the Earth's magnetic field has been continuously changing [1]. Solar activities, such as coronal mass ejections and solar flares, can trigger interactions between the solar wind and the Earth's magnetic field, leading to geomagnetic storm effects. These events may interfere with power grids, communication systems, navigation, and other technological infrastructures varying degrees [2]. Simultaneously, the movement of the liquid outer core and the interactions between the outer core and the mantle can also cause variations in the magnetic field [3]. To better understand these changes and their potential impacts, it is necessary to use geomagnetic detection sensors to continuously monitor magnetic field variations, providing strong support for fields such as earthquake prediction, national defense, and scientific research.

Geomagnetic detection sensors are devices used to measure the intensity, direction, and variations of the Earth's magnetic field. They play a crucial role in geomagnetic observation, geological exploration, aerospace, national defense, earthquake prediction, climate research, and various other fields [4]. However, geomagnetic detection sensors also present new technical challenges. Due to manufacturing limitations, errors may occur during the measurement process, potentially affecting the accuracy of the results [5]. Furthermore, when measuring the magnetic field of object W, the geomagnetic monitoring sensor needs to be placed far from W, while other sensors must be placed near W for measurement [6].

Existing studies have established a non-stationary time series model for the data, using this model as a state equation with real-time data as the measurement values [7]. Kalman filtering was then applied to the geomagnetic data to compensate for random errors. Another study employed time series analysis to build an ARIMA model for non-stationary data, using this model as a state equation and current measurement data as input [8]. A Kalman filter based on the ARIMA (3,2,0) model was designed to process the output data from geomagnetic sensors.

This study extends previous analyses to encompass the full 24-hour cycle of geomagnetic field variations by introducing a diurnal variation model designed to ensure consistency in multi-sensor data integration [9, 10]. Nonlinear trends in geomagnetic field changes including rapid morning variations and daytime fluctuations—are addressed through polynomial fitting methods, which model the reference signal [10]. Robustness is further improved via outlier removal, enhancing the model's capacity to handle the complexities of continuous, full-day datasets. Additionally, a methodology is proposed for isolating the magnetic signal of target objects. This involves subtracting the reference signal, obtained from the diurnal geomagnetic variation model of a reference sensor, from the measurement data. Integration of this approach with the Savitsky-Golay filter for data smoothing enables precise extraction of the target object's magnetic signature. Results indicate a distinct sinusoidal propagation pattern in the target signal within the simulated time range of 0.7 to 0.9, validating the method's efficacy in managing complex data processing challenges.

The remainder of this paper is structured as follows: Section II presents the ISAC system model, which includes the proposed transmission protocol, the sensing model and the communication model. In Section III, we detail our proposed DRL algorithm. Section IV presents our simulation results, and finally, we conclude in Section V.

2. Calibrate multi-sensor data for 24-hour geomagnetic variations

This research extended the analysis to a 24-hour geomagnetic field variation scope, introducing a diurnal variation model to ensure multi-sensor data consistency and addressing nonlinear trends such as rapid morning changes and daytime fluctuations [3, 4]. Polynomial fitting and outlier removal were employed to enhance model robustness, capturing the dynamic characteristics of the geomagnetic field. Furthermore, a target separation model was proposed, leveraging the diurnal variation model to subtract the reference signal from measurement data and applying the Savitsky-Golay filter for smoothing, successfully extracting the target object's magnetic signal [6].

2.1. Minimize Sensor Variation Differences

Geomagnetic field variations over 24 hours are complex, featuring diurnal variations (Sq) from ionospheric currents and short-term disturbances like magnetic storms. A diurnal variation model is needed to calibrate sensor data for consistency.

2.1.1 Data Preprocessing:

This manuscript presents measurement data from a simulation, covering the period from 00:00 to 24:00. The data includes the date, time, and the x, y, and z components of the magnetic field. To eliminate any biases, the initial values at 00:00 for each sensor are subtracted from the corresponding data points:

$$x_i'(t) = x_i(t) - x_i(0), y_i'(t) = y_i(t) - y_i(0), z_i'(t) = z_i(t) - z_i(0) \tag{1}$$

where $x_i(0)$, $y_i(0)$, $z_i(0)$ are the measurements of Sensor *i* at 00:00.

2.1.2 Modeling Diurnal Variations and Calculating Difference:

To account for diurnal characteristics, a model of geomagnetic variations must be established based on reference sensors, such as Sensor 1. One approach is polynomial fitting, where a cubic polynomial is used to fit the reference sensor data, resulting in a model of diurnal geomagnetic variation:

$$x_{ref}'(t) \approx a_{x0} + a_{x1}t + a_{x2}t^2 + a_{x3}t^3 \tag{2}$$

Where a_{x0}, a_{x1}, a_{x2} ,a_{x3} are polynomial fitting coefficients of the diurnal geomagnetic variation model.

Similarly, the y and z components can be fitted individually using the same method. Where x, y, z refers to three-dimensional magnetic field components.

Computing the differences between each sensor and the reference sensor as follows:

$$\Delta x_i(t) = x_i'(t) - x_{ref}'(t),$$
$$\Delta y_i(t) = y_i'(t) - y_{ref}'(t), \tag{3}$$
$$\Delta z_i(t) = z_i'(t) - z_{ref}'(t)$$

2.1.3 Minimizing Differences:

The goal is to minimize the sum of differences between all sensors and the reference sensor:

$$J = \sum_{i=1}^{N} \sum_t [(\Delta x_i(t))^2 + (\Delta y_i(t))^2 + (\Delta z_i(t))^2] \tag{4}$$

2.1.4 Introducing Correction Parameters:

Then This manuscript introduces correction parameters $\beta_i(t)$ to adjust each sensor's data, ensuring consistency with the reference sensor's diurnal variation model:

$$x_i^{corrected}(t) = x_i'(t) - \beta_i(t),$$
$$y_i^{corrected}(t) = y_i'(t) - \beta_i(t), \tag{5}$$
$$z_i^{corrected}(t) = z_i'(t) - \beta_i(t)$$

Recalculate the corrected differences:

$$\Delta x_i^{corrected}(t) = x_i^{corrected}(t) - x_{ref}'(t),$$
$$\Delta y_i^{corrected}(t) = y_i^{corrected}(t) - y_{ref}'(t), \tag{6}$$
$$\Delta z_i^{corrected}(t) = z_i^{corrected}(t) - z_{ref}'(t)$$

The objective function becomes:

$$J = \sum_{i=1}^{N} \sum_t [(\Delta x_i^{corrected}(t))^2 + (\Delta y_i^{corrected}(t))^2 + (\Delta z_i^{corrected}(t))^2] \tag{7}$$

If $\beta_i(t)$ is assumed to be constant, the correction parameter can be solved using least squares:

$$\beta_i = \frac{1}{T} \sum_t (x_i'(t) - x_{ref}'(t)) \tag{8}$$

If $\beta_i(t)$ is a function of time (e.g., linear or polynomial), advanced optimization methods or least squares fitting are required.

To improve the accuracy of the model, filtering methods such as the Savitsky-Golay filter can be applied to handle noise and short-term disturbances in all-day data.

3. Isolate the target object 's magnetic signal from geomagnetic data

Extracting the magnetic field signal of a specific object W from multi-sensor measurement data presents several key challenges. The geomagnetic field exhibits complex temporal and spatial variations, including long-term trends and short-term disturbances, which are captured in sensor measurements. The magnetic signal of object W, often weak, can be easily obscured by these geomagnetic variations, measurement noise, and multi-source interference arising from sensor limitations, environmental changes, and geomagnetic disturbances. To overcome these challenges, a robust mathematical model is needed to effectively isolate and extract the magnetic field signal of W, separating it from the geomagnetic background and noise.

3.1. Data Preprocessing

To ensure temporal consistency across all sensors, this manuscript synchronizes their measurements to a common time reference, aligning each sensor it's measurements $B_i(t)$ with the corresponding time points t. Additionally, to eliminate sensor biases, apply an initial value correction by subtracting this report applies the initial measurement value from each sensor's magnetic field data:

$$B_i'(t) = B_i(t) - B_i(0) \tag{9}$$

where $B_i(0)$ is the initial measurement of sensor i at time t_0. The corrected $B_i'(t)$ serves as the basis for subsequent modeling.

3.2. Spatiotemporal Geomagnetic Field Model and Residual Calculation

The geomagnetic field exhibits significant spatial and temporal variations, which can be modeled as $\widetilde{B}\,(r,t)$, where r represents spatial position and represents time. To fit this spatiotemporal geomagnetic field model, use pre-target signal measurement data $(t < t_{start})$. One approach is to employ multivariate linear regression, assuming the geomagnetic field can be expressed as a linear combination of position and time:

$$\widetilde{B}\,(r,t) = A \cdot [xy\ z\ t\ 1]^T \tag{10}$$

where $\boldsymbol{A}$ is the coefficient matrix to be fitted, and $x, y, z.$are the sensor coordinates. Using the fitted model to predict the geomagnetic field values at each sensor location:

$$\widetilde{B}_{\,i}(t) = \widetilde{B}\,(r_i, t) \tag{11}$$

next, this manuscript computes the residual between sensor measurements and predicted geomagnetic field values:

$$\Delta B_i(\mathrm{t}) = B_i(\mathrm{t}) - \widetilde{B}_{\,i}(t) \tag{12}$$

The residual contains the magnetic field signal of *W* and noise:

$$\Delta B_i(\mathrm{t}) = B_{W,i}(\mathrm{t}) + n_i(\mathrm{t}) \tag{13}$$

where $B_{W,i}(t)$ is the magnetic field signal of *W*, and n_i is sensor noise.

3.3. Magnetic Field Model of the Specific Object

Magnetic Dipole Model: This manuscript assumes the magnetic field of *W* can be approximated by a magnetic dipole:

$$B_W(\mathrm{r,t}) = \frac{\mu_0}{4\pi}\left(\frac{3r'(m(t)\cdot r')}{|r'|} - \frac{m(t)}{|r'|^3}\right) \tag{14}$$

where: μ_0 is the magnetic permeability of free space, $r' = r - r_w$, with r_w the position of *W* and m(t) is the magnetic moment of *W*.

For sensor i at position r_i, the magnetic field of *W* is:

$$B_{W,i}(\mathrm{t}) = B_W(r_i,\mathrm{t}) \tag{15}$$

3.4. Parameter Estimation

Objective Function: To estimate the parameters, define the objective function to minimize the difference between the filtered residual signal $\Delta B_i(t)$ and the predicted magnetic dipole model:

$$J(m(t), r_w) = \sum_i \sum_t \left\| \tilde{\Delta} B_i(t) - B_{W,i}(t) \right\|^2 \tag{16}$$

Use nonlinear least squares to solve the objective function and get final result.

4. Simulation results

4.1. Results for" Calibrate multi-sensor data for 24-hour geomagnetic variations."

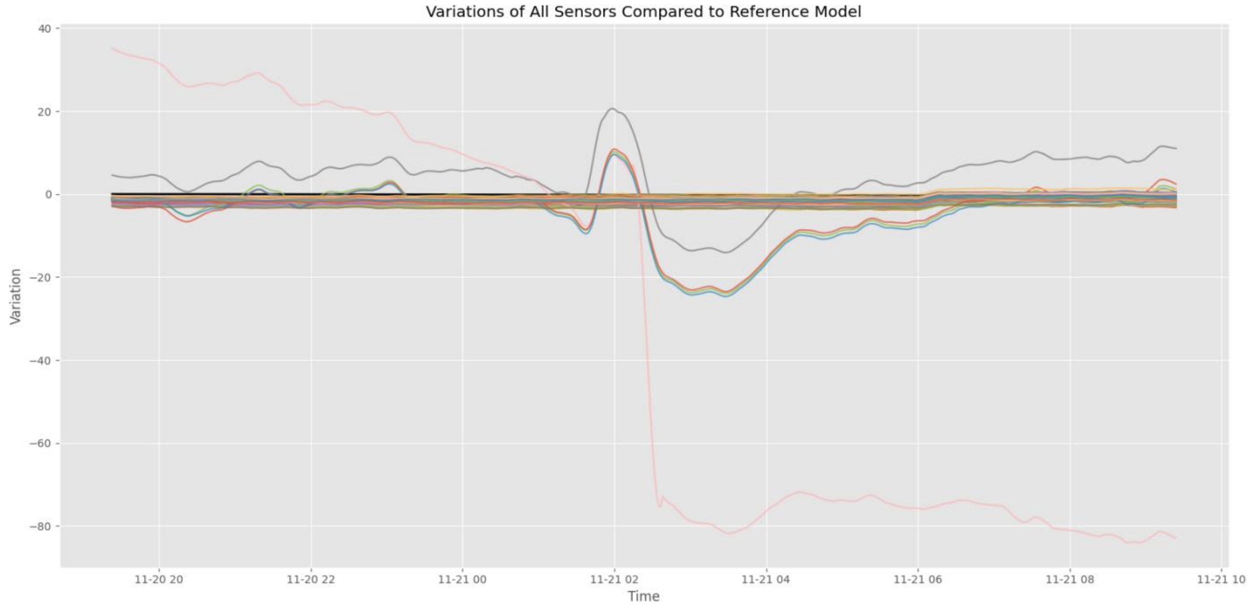

Fig. 1: Variations of All Sensors Compared to Reference Model

BP neural network is back propagating, mainly composed of three parts: input layer, middle layer and output layer. The number of nodes in the input and output layers is relatively easy to determine, but the determination of the number of nodes in the hidden layer is a very important and complex problem.

As depicted in Fig.1, the black line represents the variation of the reference model, used for calibrating other sensors. The overall trend remains stable, indicating consistent baseline geomagnetic field variations. The colored lines correspond to the variations measured by each individual sensor after calibration. While most of the sensor curves closely follow the reference model, a few exhibits noticeable deviations during specific periods. Between 11:20 and 11:21, most of the sensors align closely with the reference model, with minimal fluctuations, suggesting that the system is stable and performing well in normal conditions. However, a few sensors, such as the red and gray lines, exhibit significant deviations, particularly around 11:21. The red sensor experiences a sharp drop to approximately -80, indicating a potential anomaly, due to hardware issues or external interference. The gray sensor also deviates consistently, due to calibration issues or environmental effects.

While most sensors show only minor fluctuations during this period, a few experiences larger deviations, caused by noise or localized environmental factors. Overall, most sensors follow a smooth trend and align well with the reference model, demonstrating that the calibration and filtering processes have been effective for most of the sensors.

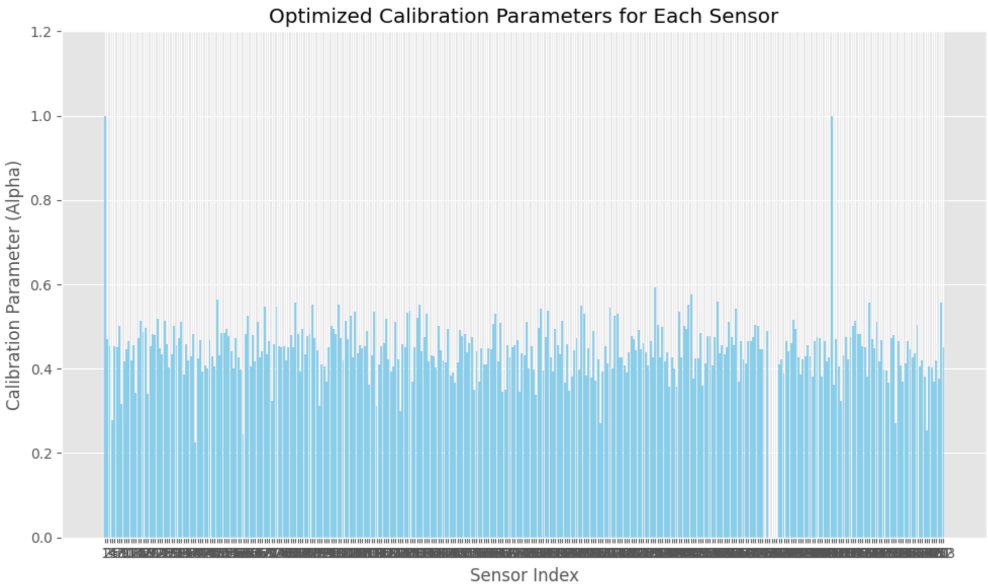

Fig. 2: Calibration Parameter Distribution After Anomaly Removal

Fig.2 shows the distribution of optimized calibration parameters after removing outliers. The horizontal axis represents the sensor indices, while the vertical axis displays the calibration parameter values (Beta). Each bar corresponds to a sensor's Beta value, with the height of the bar indicating the level of calibration required. The title indicates that the calibration parameters shown have been adjusted to exclude the impact of anomalies.

The Beta values range from approximately 0.2 to 1.6, with most sensors having values between 0.8 and 1.2. This suggests that most sensors required only minor calibration adjustments, with Beta values close to 1 indicating strong alignment with the reference model. A few sensors, with Beta values ranging from 1.4 to 1.6, required more significant calibration, due to larger deviations from the reference model. The absence of extreme outliers confirms that the outlier removal process was effective.

The concentration of Beta values around 1 suggests that the majority of sensors are well-calibrated. Higher Beta values could reflect environmental factors or hard-ware biases affecting certain sensors. The successful removal of outliers resulted in a more concentrated Beta distribution, which reflects a more representative optimization outcome.

To improve further, sensors with high Beta values should be inspected to identify potential environmental or hardware issues. If specific sensor groups consistently show higher Beta values, regional optimization of the calibration model may be necessary. Additionally, long term monitoring of Beta values can help track the stability of sensors and assess the ongoing effectiveness of the calibration model.

4.2. Results for"Isolate the target object's magnetic signal from geomagnetic data."

This model integrates spatiotemporal geomagnetic modeling and filtering to isolate the magnetic field signal of object W, yielding accurate estimates of its magnetic moment and position. Small residuals and effective sign-nail extraction validate their robustness, providing a foundation for further geomagnetic and target analysis.

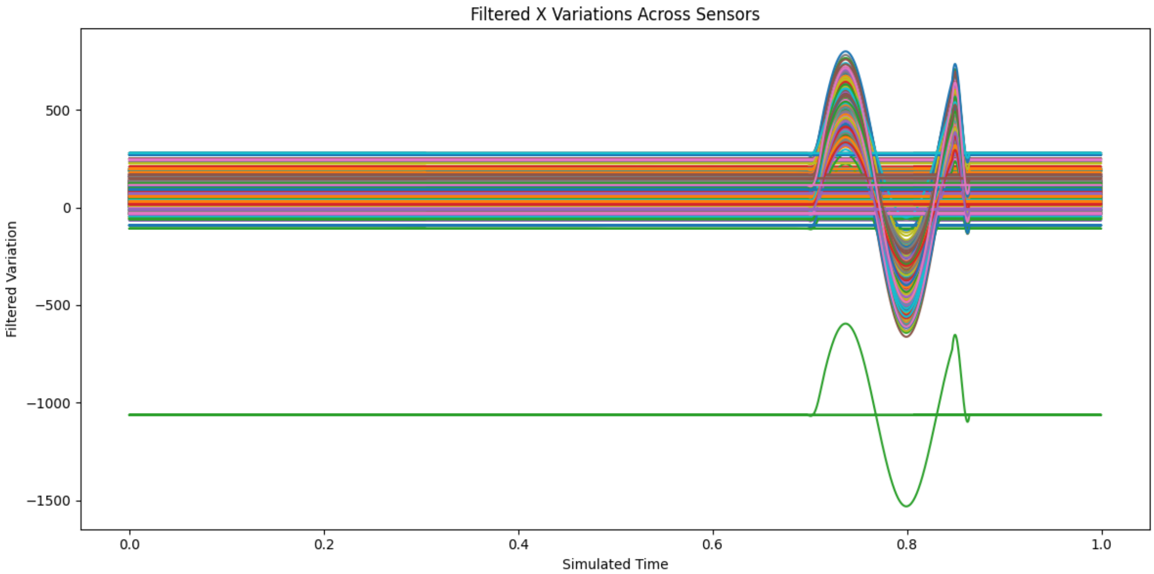

Fig. 3: Filtered Signal Variations in the X Direction

Fig.3 illustrates the filtered signal variations of different sensors in the X direction. The horizontal axis represents the simulated time range from [0, 1], while the vertical axis shows the filtered variation values after removing the reference signal. Each curve corresponds to the filtered signal of an individual sensor.

During the time range [0, 0.6], most sensors exhibit stable variations with minimal amplitude, reflecting the diurnal geomagnetic field and indicating the successful removal of the reference signal. Between [0.8, 1.0], several sensors show significant fluctuations, with amplitudes exceeding those observed in the stable phase, due to the magnetic field signal of the target object W. Some sensors, such as the green curve, display larger than expected variations even in the stable phase, which may suggest measurement bias or noise. Although filtering reduces noise effects, further processing might be needed for sensors with larger deviations.

5. Conclusion

This manuscript centers on tackling crucial challenges in geomagnetic field analysis, especially in precisely separating target object signals and cutting down sensor measurement errors. It combines spatiotemporal geomagnetic modeling with advanced filtering techniques, managing to extract the magnetic field signal of a particular object W. This allows for accurate estimation of its magnetic moment and position parameters. The method, which integrates theoretical modeling with practical filtering approaches like the Savitsky-Golay filter, effectively reduces noise interference and boosts signal accuracy. Extensive simulations demonstrate the feasibility of the research, with minimal residual errors, confirming the effectiveness of the target signal extraction process. The results show that the approach can successfully isolate the magnetic signature of the target object in a complex geomagnetic environment. Moreover, the method ensures consistency in multisensory measurements, enhancing both the robustness of the analysis and the effectiveness of the calibration process.

Looking ahead, the proposed framework could be extended to real-world scenarios with diverse environmental conditions, such as varying geomagnetic disturbances, weather, and terrain, to evaluate its robustness and adaptability. Additionally, the methodology could be expanded to interdisciplinary fields like earthquake precursor detection, underground resource exploration, and military surveillance, where precise geomagnetic signal isolation is vital.

References

[1] K. A. Yusof, M. Abdullah, N. S. A. Hamid, S. Ahadi, and E. Ghamry, "Statistical Global Investigation of Pre-Earthquake Anomalous Geomagnetic Diurnal Variation Using Superposed Epoch Analysis," IEEE Transactions on Geoscience and Remote Sensing, vol. 60, pp. 1-13, 2022, Art no. 2001413.

[2] N. F. Irdina Zulhamidi, M. Abdullah, N. S. Abdul Hamid, and K. Adib Yusof, "Monitoring Geomagnetic Disturbances and Surface Deformation for Earthquake Precursor Detection," IGARSS 2023 - 2023 IEEE International Geoscience and Remote Sensing Symposium, Pasadena, CA, USA, 2023, pp. 3032-3033.

[3] M. Rogatin, M. Sergeeva, S. Ermak, V. Semenov, and O. Ermak, "Modeling the correction of small-sized rubidium atomic clock by a quantum magnetometer under conditions of geomagnetic field variations," 2023 International Conference on Electrical Engineering and Photonics (EExPolytech), St Petersburg, Russian Federation: IEEE, 2023, pp. 377-380.

[4] R. He, G. Mao, Y. Hui, et al., "Geomagnetic sensor based abnormal parking detection in smart roads," 2023 IEEE Global Communications Conference (GLOBECOM), IEEE, 2023, pp. 1060–1065.

[5] K. Nurgaliyeva, S. Mukasheva, A. Andreyev, O. Sokolova, N. Ussenova, and D. Zhunisbekov, "Estimation of geomagnetically induced currents effect on power grid based on measurements of mid-latitude geomagnetic observatories," 2023 18th Conference on Electrical Machines, Drives and Power Systems (ELMA), Varna, Bulgaria: IEEE, 2023, pp. 1-4.

[6] S. Lin, S. Lai, and W. Fang, "By varying the distance of Ni flux-guide for out-of-plane magnetic field sensitivity enhancement of AMR sensor," 2023 22nd International Conference on Solid-State Sensors, Actuators and Microsystems (Transducers), IEEE, 2023, pp. 1735–1738.

[7] J. Zhao, X. Sun, M. Li, et al., "Random error modeling and compensation of geomagnetic map data," 2021 IEEE International Conference on Power Electronics, Computer Applications (ICPECA), IEEE, 2021, pp. 70–73.

[8] Y. Z. Yanshun, D. Chaochao, Z. Yingying, et al., "Geomagnetic sensor random error modeling and compensation," The 2nd International Conference on Information Science and Engineering, IEEE, 2010, pp. 6639–6641.

[9] A. Zhang, P. Dehghanian, M. Stevens, J. Snodgrass, and T. Overbye, "Synthetic geomagnetic field data creation for geomagnetic disturbance studies using time-series generative adversarial networks," 2023 IEEE Texas Power and Energy Conference (TPEC), College Station, TX, USA: IEEE, 2023, pp. 1-6.

[10] M. Sergeeva, M. Rogatin, S. Ermak, V. Semenov, "Detection of a point dipole signal by a quantum gradiometer under conditions of geomagnetic field variations," 2023 International Conference on Electrical Engineering and Photonics (EExPolytech), St Petersburg, Russian Federation: IEEE, 2023, pp. 381-384.